

# Characterization of Different Surface Layers Produced by Solid Boron-Nitro-Carburizing Thermochemical Treatment on AISI 1020

Alexandre Galiotto<sup>a,b,\*</sup>, Ariane Rocha Rosso<sup>b</sup>, Elisangela Aparecida dos Santos de Almeida<sup>b</sup>,

Anael Preman Krelling<sup>c</sup>, Júlio César Giubilei Milan<sup>b</sup>, César Edil da Costa<sup>b</sup>

<sup>a</sup>Instituto Federal de Santa Catarina (IFSC), campus Jaraguá do Sul, Rua dos Imigrantes, 455, Rau, CEP 89254-430, Jaraguá do Sul, SC, Brasil

<sup>b</sup>Programa de Pós-Graduação em Ciência e Engenharia de Materiais - PGCEM, Centro de Ciências Tecnológicas – CCT, Universidade do Estado de Santa Catarina (UDESC), Campus Prof. Avelino Marcante, Rua Paulo Malchitzki, Zona Industrial Norte, CEP 89225-100, Joinville, SC, Brasil

<sup>c</sup>Instituto Federal de Santa Catarina (IFSC), Campus Joinville, Rua Pavão, 1377, Costa e Silva, CEP 89220-618, Joinville, SC - Brasil

Received: May 02, 2019; Revised: July 10, 2019; Accepted: August 25, 2019

The aim of this study is to obtain and characterize surface layers on low carbon steel with the pack boron-nitro-carburizing process. Different mixtures of commercial powders (Turbonit<sup>®</sup> and Ekabor<sup>®</sup>) were used to investigate the case properties, microstructure and phases formation on AISI 1020 steel. A series of experiments were conducted in solid medium with powders blend, with weight proportions of 0/100;25/75;50/50;75/25;100/0 at temperatures of 1000 and 1100° C for 2 and 10 hours. Roughness measurement of all treated specimens was assessed to compare with pre-treatment condition. Hardness profile and comparative analysis of phase structure, morphology and composition was carried out to treatment conditions. Optical microscopy shows differences on layers surface, depth and microstructure case - diffusion zone. Results found indicated that for the same treatment time and temperature, hardness was changed, but the diffusion case depth was kept similar. DRX and XPS indicated the formation of boron nitride after certain treatments.

**Keywords:** Pack process, boron-nitro-carburizing, boron nitride.

## 1. Introduction

The industrial development stimulated the search for high performance materials. Surface engineering promotes the possibility of changing materials properties where they are most needed. Among the surface engineering processes are mechanical treatments<sup>1</sup>, thermal, diffusion treatments<sup>2</sup>, and a wide range of surface coating technologies<sup>3-5</sup>.

Among the diffusional treatments, the addition of carbon (carburizing)<sup>6-9</sup>, nitrogen (nitriding)<sup>10-13</sup> or boron (boronizing)<sup>6,14-17</sup> to the steel surface, which can be performed by solid<sup>11,12,14-17</sup>, liquid<sup>6,7</sup>, gas<sup>11,13</sup> and plasma techniques<sup>11,18,19</sup> improving wear and corrosion resistance of engineering components. Processes limitations and optimizations can be reached by the combination of different thermochemical treatments that can be performed progressively or simultaneously. These treatments are known as Carbonitriding<sup>7,19-22</sup>, Nitrocarburizing<sup>10,23-26</sup>, Borocarburizing<sup>27,28</sup> or Boronitriding<sup>29-34</sup>. A transition zone is formed between the superficial hard layer and the soft substrate - a diffusion zone, were atoms interstitially dissolved in matrix improve fatigue resistance. Furthermore, these treatments may also form a compound layer in the surface. The compound layer consists of two or more phases that provides structural improvement, and increases mechanical, wear and corrosion resistances.

Different routes and methods can be used as observed in literature. For example, samples can be first carbonitrided and then boronized, using two-temperature stage process<sup>35</sup>.

Alternative processes can also be used, Zheng Ke Quan and Zhakg Si Yu<sup>36</sup> used CO<sub>2</sub> laser as a heat source for the treatment of a metallic surface painted with organic adhesives and paste containing carbon (C), urea ((CO(NH<sub>2</sub>)<sub>2</sub>), and boron carbide (B<sub>4</sub>C). Plasma electrolytic saturation (PES) was used to produce a boron-carbonitrided nanocrystalline structure<sup>26</sup>.

This work aims to study the phases' formation and microstructure modification of 1020 steel caused by pack thermochemical treatments. Different mixture proportions of commercial powders (Turbonit<sup>®</sup> K-20 and Ekabor<sup>®</sup> as carbon/nitrogen and boron carriers) were used. Treatments were performed in two different temperatures (1000° C and 1100° C) with two different times (2 h and 10 h). The phases formed were characterized by optical microscopy, microhardness, X-ray diffraction (XRD) and X-ray photoelectron spectroscopy (XPS).

## 2. Experimental Procedure

AISI 1020 steel was used in this study. The discs samples (12.5 mm diameter x 10 mm height) were obtained from a cylindrical bar. Samples were grinded and Ra roughness was acquired. Three roughness measurements were performed in each face. Samples were ultrasonically cleaned before the thermochemical treatments. Ekabor<sup>®</sup> 1V2 was used as boriding agent. Its composition is approximately 5 %w B<sub>4</sub>C, 5 %w KBF<sub>4</sub> e 90 %w SiC<sup>37,38</sup>. Approximately 65% of the Ekabor powder particles are smaller than 105 µm, 40% of which are in the range of 53 to 105 µm.

\*e-mail: [galiotto@ifsc.edu.br](mailto:galiotto@ifsc.edu.br)

Turbonit® K-20 was used as the nitrogen carrier, its stoichiometric formula is  $\text{Fe}_4\text{KCN}^{11}$ . CHN Elemental Analysis of Turbonit® K-20 showed approximately, 61 %w carbon, 2.5 %w hydrogen and 3.5 %w nitrogen. Turbonit is granulated in form of rods, (approximately 6.75 mm diameter x 10 mm to 20 mm length). This granulated was milled to powder until 70% of the particles were larger than 105  $\mu\text{m}$ , 50% of which are larger than 250  $\mu\text{m}$ , but smaller than 350  $\mu\text{m}$ . Stainless steel containers measuring 50 mm diameter and 180 mm height were used to pack specimens and mixtures. Three samples were conditioned in the container covered with a minimum of 15 mm of powder. Ekabor®/Turbonit® K-20 blend was mixed using a "Y" type mixer during 30 minutes for complete homogenization in the following weight proportions: 0/100, 25/75, 50/50, 75/25, 100/0. The granulometry distribution of the powders' mixtures is shown in Table 1.

Thermochemical treatments were carried out under atmospheric pressure in a muffle furnace with 25 liters, (chamber volume of 400 mm X 250 mm X 250 mm). A heating rate of 20° C/min was used and cooling was performed in air. In addition, the volume occupied by the container must not exceed 60% of the chamber volume<sup>34</sup>. As each container occupies approximately 1.5 liters, 5 tubes will be used and the five mixtures will be carried out per cycle at 1000° C and 1100° C for 2 h and 10 h.

After the thermochemical treatments, roughness measurement was assessed to compare with pre-treatment condition. Measurements were obtained using

Talysurf 25 equipment. Arithmetic average roughness (Ra) was acquired using a microroughness filtering with a ratio of 25  $\mu\text{m}$ , a Gaussian filter 0.4 mm and a 0.8 mm cut-off length.

The samples were cut, sanded with SiC abrasive paper up to 600 grid, polished using 1  $\mu\text{m}$  alumina suspension and etched with a 3% Picral solution for optical micrograph analysis.

Hardness profile was acquired using a Future-Tech FM-800 tester with 100 gf load and 10 s dwell time. A minimum of 30 indentations were made on each sample condition and the hardness value is the average of at least 4 readings. The case depth (thickness) of the diffusion zone is defined as the depth where the hardness is at least 10% higher than the core hardness.

Phases and layers obtained with treatments were analyzed and identified by X-ray diffraction using Cu-K $\alpha$  radiation, scan step 0.02° and 2 $\theta$  range of 20°-110°. X-ray photoelectron spectroscopy (XPS) was used to confirm phases formed on the surface of the samples. The X-Ray spot size was set to 400  $\mu\text{m}$ .

### 3. Results and Discussion

#### 3.1 Surface finish: Roughness (Ra)

In order to evaluate the effect of different thermochemical treatments on the surface finish, roughness Ra was measured before and after the treatments. Grinded samples roughness (Ra) was 0.35  $\pm$  0.08  $\mu\text{m}$ . Roughness values of all the conditions studied are presented in Fig. 1. In general, roughness increases after thermochemical treatments.

**Table 1.** Granulometry distribution of the powders' mixtures (% w).

range [ $\mu\text{m}$ ]	0E_100T	25E_75T	50E_50T	75E_25T	100E_0T
350 > 250	50	41.375	32.75	24.125	15.5
250 > 105	20	19.375	18.75	18.125	17.5
105 > 53	15	21.625	28.25	34.875	41.5
< 53	15	17.625	20.25	22.875	25.5

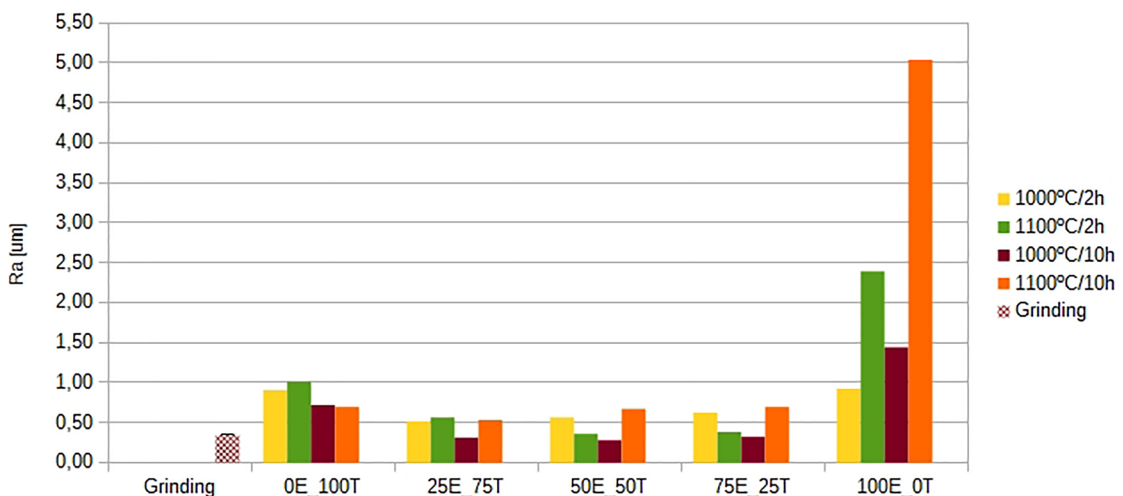


**Figure 1.** Comparative roughness values of the samples before/after thermochemical treatments

Variance analysis (ANOVA) shows that roughness parameter Ra is the same for grinded samples and treated samples at the following conditions: 50E\_50T 1000° C/10h, 50E\_50T 1100° C/2h and 75E\_25T 1100° C/2h. Borided samples (treated only with Ekabor) suffered great roughness variation with time and temperature. Higher temperatures and longer treatment times produce rougher surfaces, reaching Ra = 4.60 µm for the 100E\_0T 1100° C/10h condition. This roughness variation can be explained by the formation and growth of boride crystals on the surface.

The growth of this borides crystals structure is responsible for the increase in roughness for smooth surfaces<sup>39,40</sup>. The growth of the borides layer is a controlled diffusion process with a highly anisotropic nature. The boride crystals tends to grow along a direction of minimum resistance, perpendicular to the external surface<sup>41</sup>.

In the conditions treated with Turbonit® K20 only, there was an increase of the roughness (Ra) to approximately 0.8 µm, according ANOVA all the samples treated with Turbonit only, presented the same roughness value. It means that temperature and time did not affect roughness value in this composition condition. In the intermediate range, with mixture variations (25, 50 and 75), the same was observed; roughness values did not change with time and temperature considering any of the compositions.

### 3.2. Layer hardness and microstructure

Micro-hardness measurements were acquired from the surface to the bulk, in order to verify hardness variations between the layers, total case depth, and matrix hardness.

Figs. 2 and 4 show the comparative profile microhardness of the samples. Borided samples (100E\_0T) at 1000 °C for 2 hours presented a microhardness value of approximately 1200 HV. The 1000 °C\_10h and 1100 °C\_2h (0E\_100T) conditions presented similar behavior, comparing the curves. The maximum hardness obtained in these conditions is 1000 HV. By the curves, it is possible to observe that the increase in temperature for 2 hours treatment promoted an increase in case depth. In the 0E\_100T at 1100° C for 2 hours condition the hardness on the nearest edge of the layer could not be measured, due to the porosity/high roughness (Ra = 2.4 µm) of this layer. Measurements from hardness begun from 50 µm distance from the surface.

Borided conditions (100E\_0T) presented a borided layer with saw-tooth diffusion front and their surfaces are rough and porous. Increasing temperature and time, saw-tooth morphology is less pronounced and the average roughness (Ra) increases varying from 0.92 to 5.04 µm, in agreement with surface finish, showed in Fig. 1. The saw-tooth morphology depends not only on chemical composition of treated steel, but also on boriding temperature and time<sup>6</sup>.

In the microhardness profile of 100E\_0T at 1100° C\_10h condition, it is possible to identify four distinct zones. This condition presented a different behavior considering hardness profile and the microstructural image shows different zones comparing to the others. These zones are shown in the cross-section microstructure image of Fig. 3(d). The thickness of the layers observed in Fig. 3(d), from the outermost to the innermost layer, are in the range of 115-125 µm (dark and porous zone), 72-77 µm (compact zone), 120-140 µm

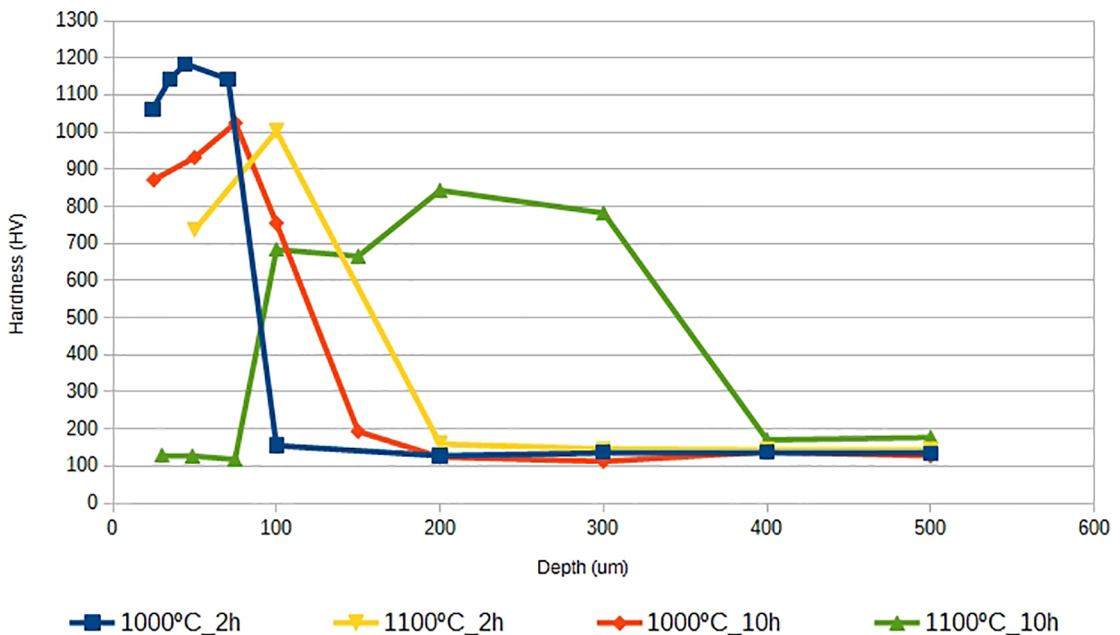


Figure 2. Hardness profiles of the borided AISI 1020 steel at 1000° C / 1100° C for 2h and 10h

(saw-tooth zone) and a diffusion zone reaching 1000  $\mu\text{m}$  and hardness varying from 170 to 180 HV. The matrix hardness average of this condition was about 145 HV.

The mixtures hardness profiles have similar behavior to Turbonit<sup>®</sup> according to graphs of Fig. 4. Initially, the hardness profile rises, reaching a maximum hardness value then decreases until the hardness of steel core. According Dal'Maz Silva *et al.*<sup>19</sup> decarburizing should be taken into account in carbonitriding treatments and the hardness peak under the surface is related to the repulsion of interstitial elements themselves, i.e. carbon-carbon, nitrogen-nitrogen and nitrogen-carbon negative interacting energies.

Since these two elements interact with another in the austenite, the equilibrium with the atmosphere varies with gas composition and temperature<sup>20,21</sup>.

Microhardness analysis shows that hardness profiles vary with mixtures. Hardness decreases as the amount of Turbonit<sup>®</sup> decreases and the amount of Ekabor<sup>®</sup> increases. The reactions that occur in the process depends on the kinetics and equilibrium among gas interchange reactions and the gas-metal reactions. Increasing treatment time and temperature generates an increase in case depth, underlined by the black line in the graphs. Under the same conditions of time and temperature, regardless of the mixture, the case depth is similar to Turbonit<sup>®</sup>.

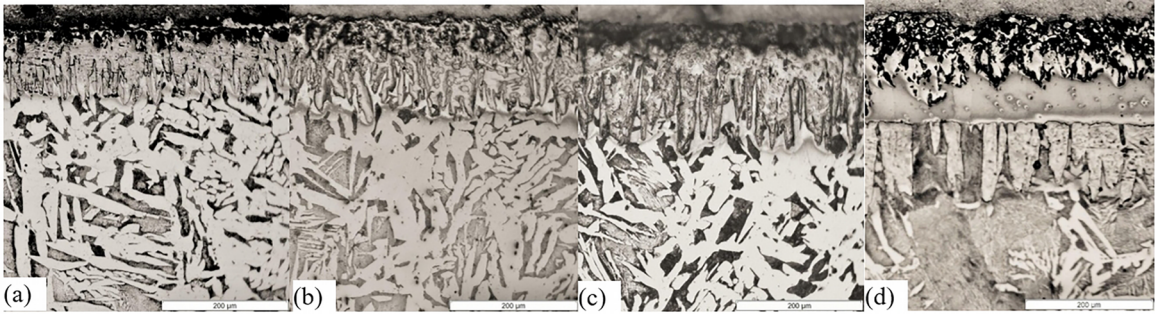


**Figure 3.** (a) cross-section optical micrograph of AISI 1020 at 1000° C for 2h, (b) cross-section optical micrograph of AISI 1020 at 1100° C for 2h, (c) cross-section optical micrograph of AISI 1020 at 1000° C for 10h, (d) cross-section optical micrograph of AISI 1020 at 1100° C for 10h.

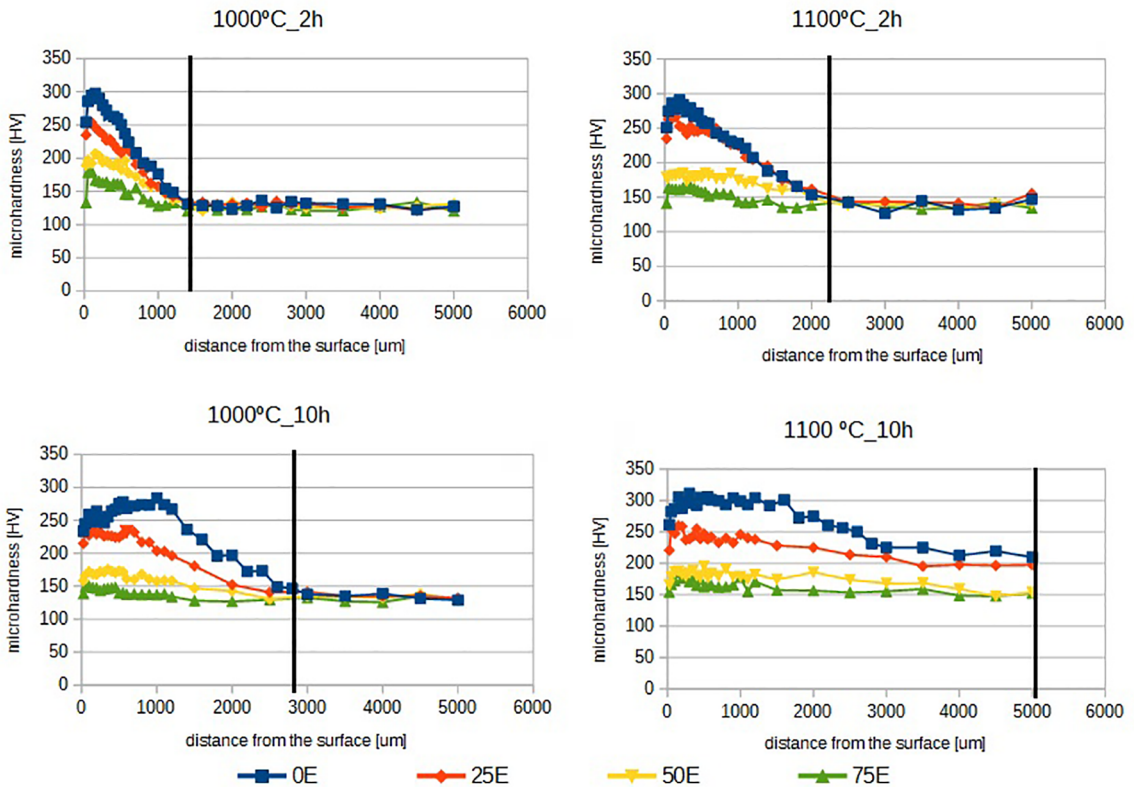


**Figure 4.** Hardness profiles of AISI 1020 steel thermochemically treated with Turbonit<sup>®</sup> and mixtures Tubonit<sup>®</sup>+Ekabor<sup>®</sup> at 1000° C/1100° C for 2 h and 10 h.

In the mixtures of 0E\_100T and 25E\_75T at 1100° C\_10 h the diffusion was so intense that reached the sample core (5 mm). The matrix average microhardness increased from 120 HV to 220 HV.

Fig. 5 shows optical micrographs of AISI 1020 steel thermochemically treated with whit Turbonit and mixtures Tubonit®+Ekabor®. For these conditions iron borides layers are not observed, only observed for 100E\_OT Fig. 2a-d.

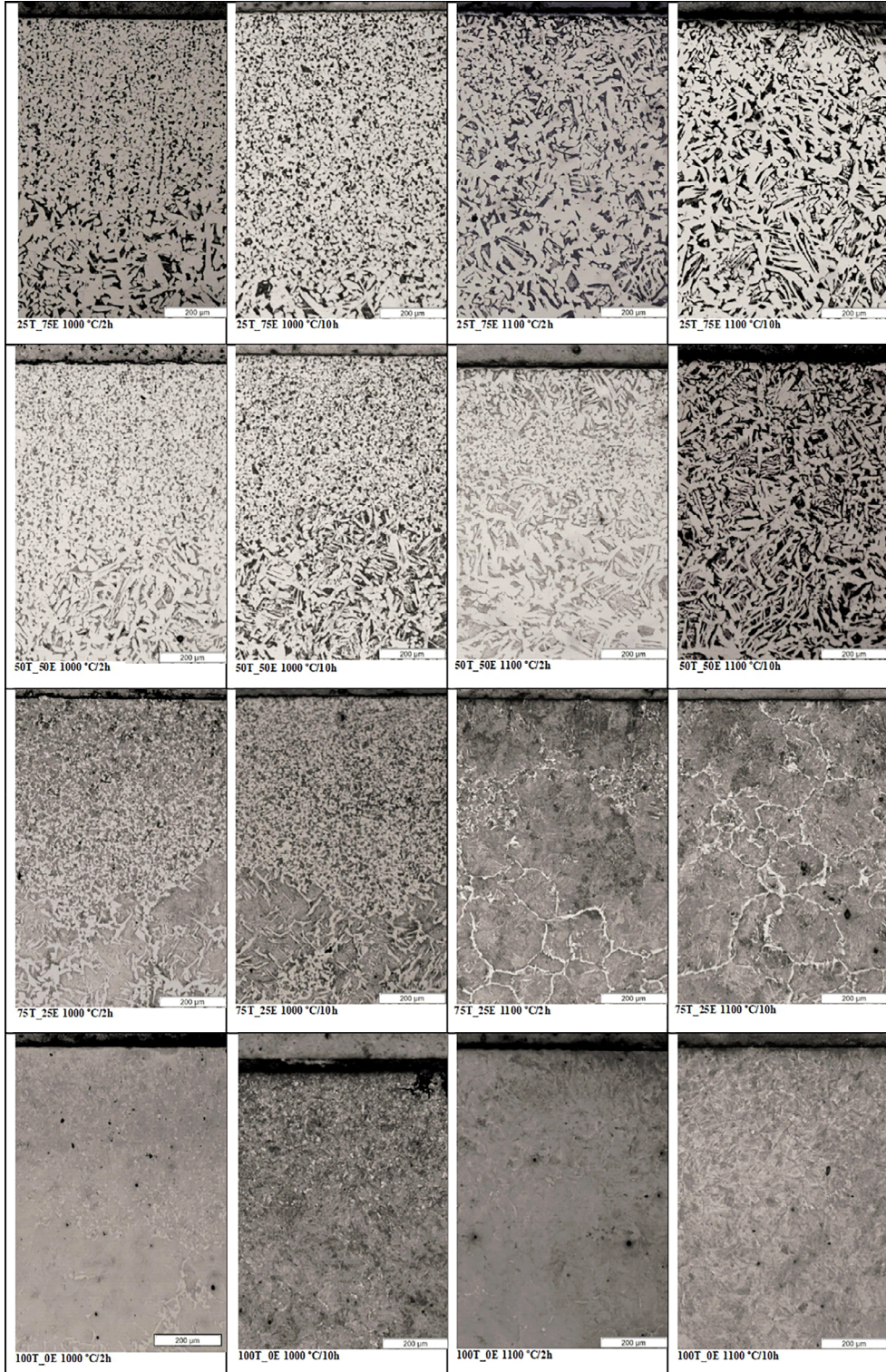


**Figure 5.** Cross-sections optical micrographs (mag. 100x) of AISI 1020 steel thermochemically treated with Turbonit® and mixtures Tubonit®+Ekabor® (2 h and 10 h at 1000° C and 1100° C).

In Turbonit®+Ekabor® mixtures at 1000° C for 2 h and 10 h, a diffusion zone with grain refinement can be seen and the fraction of pearlite increases when the amount of Turbonit increases and Ekabor® decreases in the mixtures. Stumpf and Banks<sup>42</sup> found that 10 to 30 ppm of boron enhances hardenability of steel through segregation at austenite grain boundaries and hence delays the nucleation of ferrite and pearlite. In the condition of 1100° C\_2h only some islands, sub-superficial regions are identified with grain refinement and in the condition of 1100° C\_10h there was no grain refinement.

Samples treated only with Turbonit® (100T\_0E) show perlite microstructure and the diffusion layer increases with time and temperature increase, reaching the sample core (5 mm), after 10 hours treatment at 1100° C.

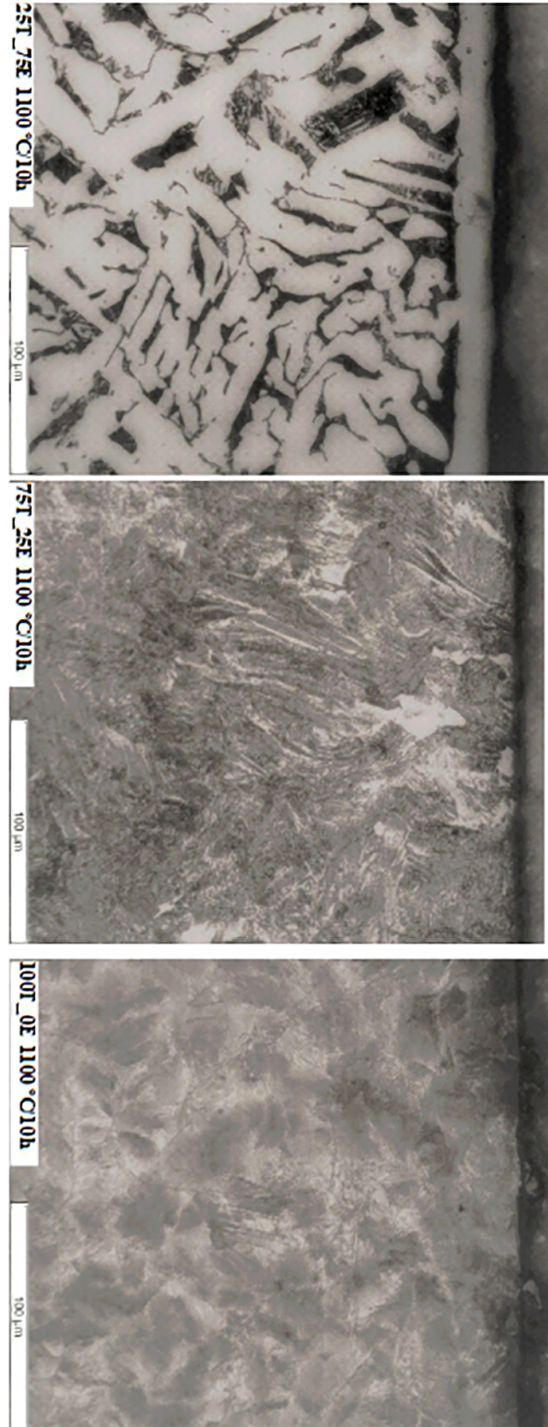
### 3.3. XPS and DRX analysis

Fig. 6 shows the different microstructures formed varying the percentage of Turbonit® and Ekabor® in the mixtures. A homogeneous and flat layer is formed in the samples treated with 25T\_75E at 1100° C for 10 h. The existence of boron nitride (BN) was verified by X-ray diffraction in Fig. 6b. The XPS analysis on the surface confirms that this layer is basically composed by 30.5%at boron, 33.5%at nitrogen, 22.5%at carbon and 8%at oxygen. In this fraction mixture (25T\_75E) treated at 1000° C for 2 h no layer is evidenced by micrography, but XPS analysis denotes elevated percentage of boron (37.5%at), nitrogen (29.5%at), carbon (23.5%at) and oxygen (6.5%at). This indicates that the boron nitrides are formed even in lower temperature and time treatments.

Even though a layer is not observed for 75T\_25E treated at 1100° C for 10 h condition, the XPS analysis indicates high amount of boron (~22%p), nitrogen (26%p) and carbon (~13.5%p). The existence of boron nitrides (BN) in the mixtures of Turbonit®+Ekabor® was verified by X-ray diffraction in Fig. 7.

Fig. 6 shows a typical eutectoid microstructure for the samples treated only with Turbonit® (100T\_0E). Fig. 8 compares surface X-ray diffraction patterns of 1020 steel substrate and AISI 1020 steel thermochemically treated with Turbonit®. The increase in time and temperature change the intensities - strongest reflections in  $2\theta = 26.8^\circ$  - refining cementite peak.

As observed in Fig. 3d, the cross-section micrograph of 100E\_0T at 1100° C\_10 h, this condition has four distinct zones. A layer-by-layer X-ray diffraction analysis was held and is showed in Fig. 9.



**Figure 6.** Cross-sections micrographs of AISI 1020 steel thermochemically treated with mixtures Turbonit®+Ekabor® and Turbonit® during 10 h at 1100° C.

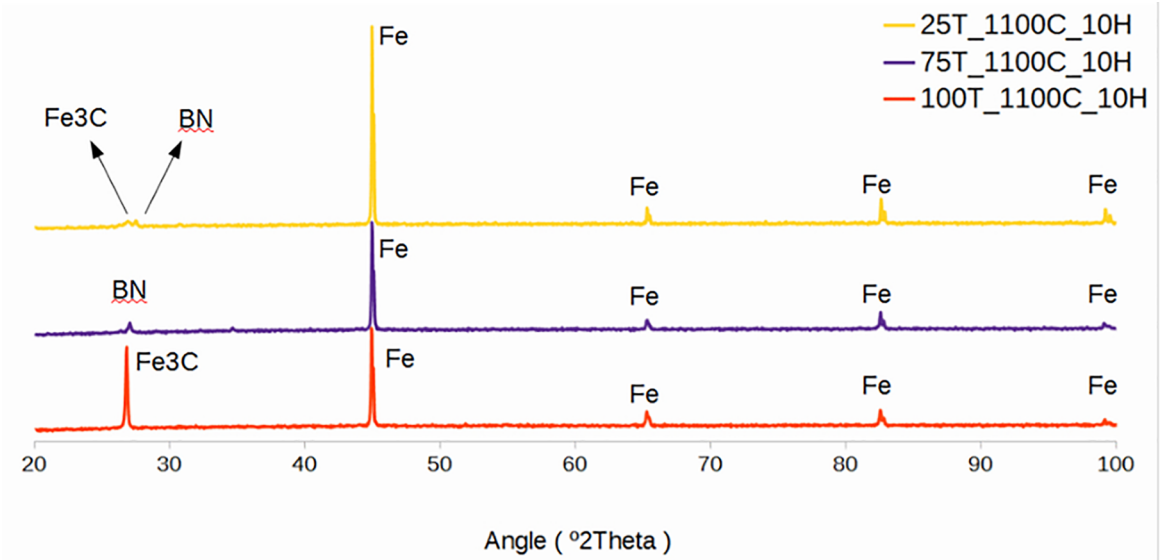


Figure 7. X-ray diffraction patterns obtained at the surface of the AISI 1020 steel thermochemically treated with mixtures Turbonit®+Ekabor® and Turbonit® during 10 h at 1100° C.

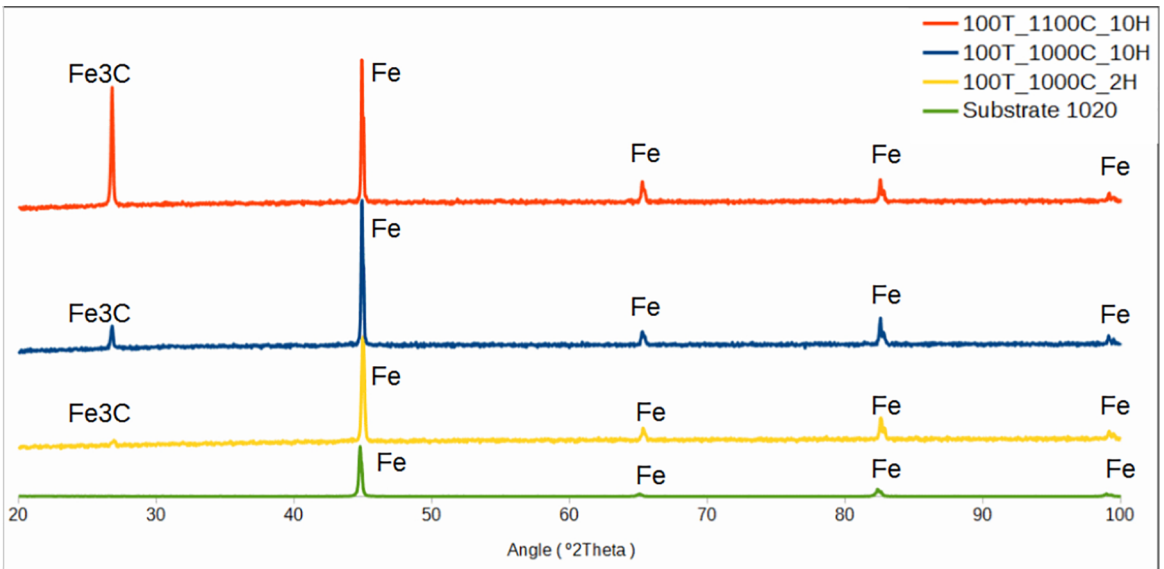
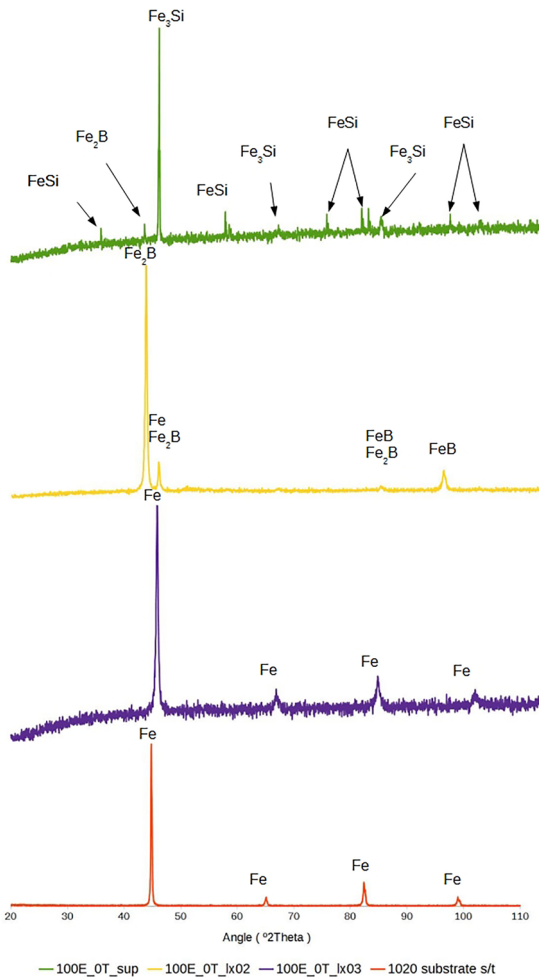


Figure 8. Comparative surface X-ray diffraction patterns of 1020 steel substrate and AISI 1020 steel thermochemically treated with Turbonit®

Fig. 9a represents X-ray diffraction of the reference AISI 1020 steel surface without treatment. X-ray diffraction of the borided surface (Fig. 9d) shows peaks of  $Fe_2B$  (01-072-1301),  $FeSi$  (01-088-1298) and  $Fe_3Si$  (00-035-0519). Similar results were found by Carbucicchio *et al.*<sup>43</sup>, when replacing  $SiC$  by  $SiN_4$  in the powder mixture.  $FeB$  and

$Fe_2B$  peaks are observed after a progressive removal material. The same peaks, in Fig.9c, are detected in layers at 150  $\mu m$  and 250  $\mu m$  below the surface. After 500  $\mu m$  material removal, X-ray diffraction analysis is similar to the pattern of AISI 1020 steel surface without treatment showing only  $Fe$  peaks.



**Figure 9.** X-ray diffraction patterns for a) 1020 steel substrate without treatment; layer-by-layer of borided AISI 1020 steel treated with Ekabor® at 1100°C for 10 h - b) and c) patterns obtained with progressive removal of material, d) borided surface

## 4. Conclusion

The study comparing thermochemical treatments using commercial nitriding/boriding powders and mixtures presents the following results:

1. It is possible to develop a boron nitride layer on AISI 1020 surface by pack process using different mixture proportions of commercial powders: Turbonit® K-20 and Ekabor® as carbon/nitrogen and boron carrier.
2. The treatment with the mixtures slightly change the surface finish and in certain conditions produce a compact and porosity free layer of boron nitride.
3. Hardness of the borided layers are higher than those obtained in the samples treated with Turbonit® K-20 and also higher than the hardness of the mixtures: Turbonit® K-20 and Ekabor®.

4. The mixtures hardness profiles have similar behavior to Turbonit®. Decreasing the amount of Turbonit® and increasing the amount of Ekabor® cause a decrease in hardness. Temperature and time do not affect significantly the maximum hardness to same fraction mixture, just the total case.
5. Boron diffusion produces a zone of refined grains in samples treated with mixtures at 1000° C for 2 h and 10 h.
6. FeSi and Fe<sub>3</sub>Si presence/growth on the surface is observed for the borided at high temperature and long time process samples (1100° C for 10 h).

The optimum treatment parameters (time, temperature and mixtures fractions) should be studied to a better understanding on the mechanisms of layers formation-reactions occurring in the process, kinetics and equilibrium among gas interchange reactions and the gas-metal reaction. The results will open new possibilities for their practical application.

## 5. Acknowledgements

This study was financed in part by the Coordenação de Aperfeiçoamento de Pessoal de Nível Superior - Brasil (CAPES) - Finance Code 001.

## 6. References

1. Fang Y, Chen X, Madigan B, Cao H, Konovalov S. Effects of strain rate on the hot deformation behavior and dynamic recrystallization in China low activation martensitic steel. *Fusion Engineering and Design*. 2016;103:21-30.
2. Almeida EAS, Krelling AP, Milan JCG, Costa CE. Micro-abrasive wear mechanisms of P/M AISI M2 steel with different surface treatments. *Surface and Coatings Technology*. 2018;333:238-46.
3. Konovalov SV, Kormyshev VE, Gromov VE, Ivanov YF, Kapralov EV, Semin AP. Formation features of structure-phase states of Cr-Nb-C-V containing coatings on martensitic steel. *Journal of Surface Investigation. X-ray, Synchrotron Neutron Techniques*. 2016;10(5):1119-24.
4. Lara LOC, Mello JDB. Influence of layer thickness on hardness and scratch resistance of Si-DLC/CrN coatings. *Tribology - Materials, Surfaces & Interfaces*. 2012;6(4):168-73.
5. Pougoum F, Qian J, Martinu L, Klemberg-Sapieha J, Zhou Z, Li KY, et al. Study of corrosion and tribocorrosion of Fe 3 Al-based duplex PVD/HVOF coatings against alumina in NaCl solution. *Surface and Coatings Technology*. 2019;357:774-83.
6. Selçuk B, Ipek R, Karamiş MB, Kuzucu V. An investigation on surface properties of treated low carbon and alloyed steels (boriding and carburizing). *Journal of Materials Processing Technology*. 2000;103(2):310-7.
7. Selçuk B, Ipek R, Karamiş MB. A study on friction and wear behaviour of carburized, carbonitrided and borided AISI 1020 and 5115 steels. *Journal of Materials Processing Technology*. 2003;141(2):189-96.

8. Edenhofer B, Joritz D, Rink M, Voges K. Carburizing of steels. In: Mittemeijer EJ, Somers MAJ, editors. *Thermochemical Surface Engineering of Steels*. Cambridge: Woodhead Publishing; 2014. p. 485-553.
9. Bepari MMA. 2.3 Carburizing: A Method of Case Hardening of Steel. In: Hashmi MSJ, editor. *Comprehensive Materials Finishing*. Amsterdam: Elsevier; 2017. p. 71-106. v. 2.
10. Mittemeijer EJ. Fundamentals of Nitriding and Nitrocarburizing. In: Dosset JL, Totten GE, editors. *ASM Handb Vol 4A: Steel Heat Treating Fundamentals and Processes*. Materials Park, OH: ASM International; 2013. p. 28. v. 4.
11. Almeida EAS, Costa CE, Milan JCG. Study of the nitrided layer obtained by different nitriding methods. *Matéria (Rio de Janeiro)*. 2015;20(2):460-5.
12. Campos-Silva I, Ortiz-Dominguez M, Elias-Espinosa M, Vega-Morón RC, Bravo-Bárceñas D, Figueroa-López U. The Powder-Pack Nitriding Process: Growth Kinetics of Nitride Layers on Pure Iron. *Journal of Materials Engineering and Performance*. 2015;24(9):3241-50.
13. Cavaliere P, Perrone A, Silvello A. Multi-objective optimization of steel nitriding. *Engineering Science and Technology, an International Journal*. 2016;19(1):292-312.
14. Uslu I, Comert H, Ipek M, Celebi F, Ozdemir O, Bindal C. A comparison of borides formed on AISI 1040 and AISI P20 steels. *Materials and Design*. 2007;28(6):1819-26.
15. Elias-Espinosa M, Silva JZ, Ortiz-Dominguez M, Hernández-Ávila J, Damián-Mejía O. Diffusional Growth Kinetics Analysis of Fe<sub>2</sub>B Layers Applied During the Coating Powder-Pack Boriding Process on an AISI 1026 Steel. *Nova Scientia*. 2015;7(14):74-101.
16. Zhong J, Qin W, Wang X, Medvedovski E, Szpunar JA, Guan K. Mechanism of Texture Formation in Iron Boride Coatings on Low-Carbon Steel. *Metallurgical and Materials Transactions A*. 2018;(1).
17. Krelling AP, Teixeira F, Costa CE, Almeida EAS, Zappelino B, Milan JCG. Microabrasive wear behavior of borided steel abraded by SiO<sub>2</sub> particles. *Journal of Materials Research and Technology*. 2018;8(1):766-776.
18. He X, Xiao H, Ozaydin MF, Balzuweit K, Liang H. Low-temperature boriding of high-carbon steel. *Surface & Coatings Technology*. 2015;263:21-6.
19. Silva WDM, Dulcy J, Ghanbaja J, Redjaïmia A, Michel G, Thibault S, et al. Carbonitriding of low alloy steels: Mechanical and metallurgical responses. *Materials Science and Engineering: A*. 2017;693:225-32.
20. Slycke J, Ericsson T. A Study of Reactions Occurring During the Carbonitriding Process. *Journal of Heat Treating*. 1981;2(2):4-19.
21. Slycke J, Ericsson T. A Study of Reactions Occurring during the Carbonitriding Process Part II. *Journal of Heat Treating*. 1981;2(2):97-112.
22. Shen DJ, Wang YL, Nash P, Xing GZ. A novel method of surface modification for steel by plasma electrolysis carbonitriding. *Materials Science & Engineering A*. 2006;458(1-2):240-3.
23. Pereloma EV, Conn AW, Reynoldson RW. Comparison of ferritic nitrocarburising technologies. *Surface and Coatings Technology*. 2001;145(1-3):44-50.
24. Somers MAJ. Nitriding and Nitrocarburizing: Current Status and Future Challenges. *Heat Treat & Surface Engineering Conference & Expo*. 2013;69-84.
25. Zarchi MK, Shariat MH, Dehghan SA, Solhjo S. Characterization of nitrocarburized surface layer on AISI 1020 steel by electrolytic plasma processing in an urea electrolyte. *Journal of Materials Research and Technology*. 2013;2(3):213-20.
26. Taheri P, Dehghanian C, Aliofkhaezai M, Rouhaghdam AS. Nanocrystalline structure produced by complex surface treatments: Plasma electrolytic nitrocarburizing, boronitriding, borocarburing, and borocarbonitriding. *Plasma Processes and Polymers*. 2007;4(Suppl 1):721-7.
27. Kulka M, Makuch N, Dziarski P, Mikołajczak D, Przystacki D. Gradient boride layers formed by diffusion carburizing and laser boriding. *Optics and Lasers in Engineering*. 2015;67:163-75.
28. Kulka M, Pertek A. Gradient formation of boride layers by borocarburing. *Applied Surface Science*. 2008;254(16):5281-90.
29. Gómez-Vargas OA, Solís-Romero J, Figueroa-López U, Ortiz-Dominguez M, Oseguera-Peña J, Neville A. Boro-nitriding coating on pure iron by powder-pack boriding and nitriding processes. *Materials Letters*. 2016;176:261-4.
30. Maragoudakis NE, Stergioudis G, Omar H, Pavlidou E, Tsipas DN. Boro-nitriding of steel US 37-1. *Materials Letters*. 2002;57(4):949-52.
31. Balandin YA. Boronitriding of die steels in fluidized bed. *Metal Science and Heat Treatment*. 2004;46(9-10):385-7.
32. Mindivan H. Effects of combined diffusion treatments on the wear behaviour of hardox 400 steel. *Procedia Engineering*. 2013;68:710-5.
33. Man WD, Wang JH, Ma ZB, Wang CX. Plasma boronitriding of WC(Co) substrate as an effective pretreatment process for diamond CVD. *Surface and Coatings Technology*. 2002;171(1):241-6.
34. Wang Y, Liu X. The Performance Study about the Boronitriding Layer in the Low Temperature. *2011 Second International Conference on Digital Manufacturing Automation*. 2011;1309-12.
35. Yan PX, Su YC. Metal surface modification by B-C-nitriding in a two-temperature-stage process. *Materials Chemistry and Physics*. 1995;39(4):304-8.
36. Quan ZK, Yu ZS. The influence of laser carbo-nitro-boriding on metallic surface properties. *Materials Chemistry and Physics*. 1990;24(3):279-85.
37. Zimmerman C. Boriding (Boronizing) of Metals. In: Dossett JL, Totten GE, editors. *Steel Heat Treating Fundamentals and Processes*. ASM International; 2013. p. 437-47. v. 4.
38. Gunes I, Ulker S, Taktak S. Plasma paste boronizing of AISI 8620, 52100 and 440C steels. *Materials and Design*. 2011;32(4):2380-6.
39. Şahin S. Effects of boronizing process on the surface roughness and dimensions of AISI 1020, AISI 1040 and AISI 2714. *Journal of Materials Processing Technology*. 2009;209(4):1736-41.

40. Jain V, Ganesh I. Influence of the pack thickness of the boronizing mixture on the boriding of steel. *Surface and Coatings Technology*. 2002;149(1):21-26.
41. Palombarini G, Carbucicchio M. Growth of boride coatings on iron. *Journal of Materials Science Letters*. 1987;6(4):415-6.
42. Waldo S, Banks K. The hot working characteristics of a boron bearing and a conventional low carbon steel. *Materials Science and Engineering A*. 2006;418(1):86-94.
43. Carbucicchio M, Casagrande A, Palombarini G. Competitive reactivity of iron towards boron and silicon in surface treatments with powder mixtures. *Hyperfine Interactions*. 1990;57(1-4):1769-74.